Carbohydrate Polymers 80 (2010) 866–873

Contents lists available at ScienceDirect

Carbohydrate Polymers

journal homepage: www.elsevier.com/locate/carbpol

Bionanocomposites of thermoplastic starch reinforced with bacterial cellulose nanofibres: Effect of enzymatic treatment on mechanical properties

Marco Aurélio Woehl [a], Carla Daniele Canestraro [b], Alexandre Mikowski [b], Maria Rita Sierakowski [a], Luiz Pereira Ramos [a], Fernando Wypych [a,*]

[a] Centro de Pesquisas em Química Aplicada – CEPESQ, Universidade Federal do Paraná, Departamento de Química, CP 19081, CEP 81531-980, Curitiba, PR, Brazil
[b] Universidade Federal do Paraná, Departamento de Física, CP 19091, CEP 81531-980, Brazil

ARTICLE INFO

Article history:
Received 1 December 2009
Received in revised form 18 December 2009
Accepted 23 December 2009
Available online 7 January 2010

Keywords:
Plasticized starch
Bacterial cellulose
Nanofibres
Nanocomposites

ABSTRACT

Acetobacter xylinum bacterial cellulose (BC) was used as reinforcement agent in glycerol-plasticized cassava starch bionanocomposites before and after treatment with *Trichoderma reesei* endoglucanases. Hydrolysis for 60 min with an enzyme loading of 10 mg of protein per gram of substrate decreased the degree of polymerization of cellulose without changing its crystallinity index or promoting a significant mass loss. However, the mechanical properties of the partially hydrolysed BC nanofibres were outstanding. The elastic modulus of the bionanocomposite (575.7 ± 166.7 MPa) was seventeen times higher than that of the starch matrix (33.4 ± 4.3 MPa) and four times higher than that of the film containing untreated fibres (140.6 ± 40.3 MPa). Likewise, the tensile strength (8.45 ± 2.35 MPa) was increased by a factor of eight in relation to the former (1.09 ± 0.39 MPa) and almost doubled in relation to the latter (4.15 ± 0.66 MPa). Hence, BC nanofibres were shown to be excellent reinforcement agents for the production of starch-based bionanocomposites.

1. Introduction

Since the discovery in the beginning of the nineties that the dispersion of clay mineral nanoparticles in a polymer matrix considerably improves its mechanical properties (Okada, Kawasumi, Kurauchi, & Kamigaito, 1987; Usuki et al., 1990, 1993), polymer based nanocomposites have been intensely studied (Tjong, 2006; Zhao, Torley, & Halley, 2008). A large number of organic and inorganic materials, such as clay minerals (Chen & Evans, 2005; Usuki et al., 1990, 1993; Wilhelm, Sierakowski, Souza, & Wypych, 2003) and lignocellulosic fibres (Malainine, Mahrouz, & Dufresne, 2005; Orts et al., 2005; Stael, Tavares, & D'Almeida, 2001) have been tested as potential sources of nanoparticles and nanofibres to be used as nanofillers. These materials have the advantage of being renewable, which means they have a much smaller environmental impact than their synthetic equivalents (Satyanarayana, Arizaga, & Wypych, 2009). Therefore, they are useful to prepare commercially viable "green products" or "eco-friendly materials".

The development of bionanocomposites depends on the use of natural resources as both the polymer matrix and the nanoscale reinforcement agent. Polylactates (Yu, Dean, & Li, 2006) and plasticized or thermoplastic starch (TPS) (Avérous, Frigant, & Moro, 2001; López-Rubio et al., 2007; Mathew & Dufresne, 2002; Ângles & Dufresne, 2000) are good examples for such applications. Since they are based on renewable resources, these materials offer several advantages over plastics derived from petrochemistry: they are biodegradable, environmentally benign, less abrasive to processing machines and non-toxic to humans and animals (Satyanarayana et al., 2009).

This work proposes the use of a much underestimated source of nanofibres, bacterial cellulose. In addition, the matrix is composed of cassava starch plasticized with glycerol. Cassava is an important source of starch in the Southern Hemisphere, but its use in composite materials is explored very little. On the other hand, the use of glycerol as a starch plasticizer has attracted considerable interest because of its increasing availability at relatively low costs, which is primarily due to the current expansion of the biodiesel industry. Bacterial cellulose nanofibres are obtained by an enzymatic treatment, which is energetically and environmentally better than the current alternatives based on mechanical disruption (Abe, Iwamoto, & Yano, 2007) or strong acid hydrolysis (Bondeson, Mathew, & Oksman, 2006).

2. Experimental

Never-dried mats of *Acetobacter xylinum* bacterial cellulose were kindly supplied by Membracel Produtos Tecnológicos Ltda. (Almirante Tamandaré, PR, Brazil). Cassava starch with 17 wt% amylose and 83 wt% amylopectin was obtained from Corn Products

* Corresponding author. Tel.: +55 41 3361 3473; fax: +55 41 3361 3186.
E-mail address: wypych@quimica.ufpr.br (F. Wypych).

0144-8617/$ - see front matter © 2010 Elsevier Ltd. All rights reserved.
doi:10.1016/j.carbpol.2009.12.045

Brasil (Balsa Nova, PR, Brazil), and glycerol was obtained in pure grade from Sigma–Aldrich (St. Louis, Missouri, USA).

The *Trichoderma reesei* endoglucanase preparation used in this study was a kind gift from Röhm Enzymes Finland Oy (currently Roal Oy). This preparation was produced with a protein content of 17.7 mg mL^{-1} and an endoglucanase activity (carboxymethylcellulase activity) of 23.73 U mg^{-1} by a genetically modified strain in which both cbh1 and cbh2 genes were deleted, using the methods described by Suominen, Mäntylä, Karhunen, Hakola, and Nevalainen (1993). Further details about the properties and the mode of action of this enzyme are described elsewhere (Ramos, Zandoná Filho, Deschamps, & Saddler, 1999; Zandoná Filho, Cancelier, Siika-Aho, & Ramos, 2003).

2.1. Enzymatic hydrolysis of the bacterial cellulose

Before hydrolysis, bacterial cellulose mats with 99.5 wt% moisture content were homogenized in a kitchen blender and kept under refrigeration in the presence of 0.1 mg mL^{-1} of sodium azide. The amount of enzymes used for hydrolysis was 10 mg of protein per gram of substrate, based on average values used to obtain cellulose nanofibres. The moisture content was always determined at 110 °C until constant weight (Henriksson, Henriksson, Berglund, & Lindström, 2007).

Dispersed fibres of bacterial cellulose were hydrolysed in 10% (vol/vol) citrate buffer (pH 4.8) at 45 °C, 150 rpm and 0.5 wt% solids concentration. Hydrolysis was performed in shake flasks for incubation times varying from 20 to 240 min. After this, the medium was immediately immersed in a boiling water bath for 5 min to inactivate the enzymes, cooled in an ice bath, centrifuged at 9000 rpm for 30 min and washed thoroughly with distilled water. The resulting fibres were stored under refrigeration for subsequent analysis and incorporation in the composite films.

The extent of enzymatic hydrolysis was evaluated by measuring the release of reducing sugars using the Somogyi–Nelson method (Chaplin & Kennedy, 1994). Bacterial cellulose hydrolysates were also characterized by high performance liquid chromatography (HPLC), using an Aminex HPX-87H column (Bio-Rad) at 65 °C with 8 mmol/L H_2SO_4 as mobile phase (Ramos & Fontana, 2004). Soluble sugars (glucose and cellobiose) were detected by differential refractometry and quantified by external calibration. The results were converted to anhydroglucose equivalents and used to calculate the total hydrolysis mass loss in relation to the dry weight of the starting material.

2.2. Characterization of the partially hydrolyzed fibres

X-ray powder diffraction (XRPD) was used to verify possible changes in crystallinity, crystalline organization and relative dimensions of the cellulose crystallites. Prior to the XRPD experiments, the moisture present in both untreated and partially hydrolysed bacterial cellulose was exchanged with *tert*-butanol using a stepwise gradient. The last washing steps were carried out with pure *tert*-butanol. The fibre suspension was centrifuged for 20 min at 10,000 rpm and the recovered fibres were lyophilized in a bench-top freeze-drier. This procedure was carried out to minimize recrystallisation of the cellulose chains during drying, with the consequent alteration in its crystallinity index (Ramos, Nazhad, & Saddler, 1993).

The X-ray powder diffraction experiments were performed in a Shimadzu XRD 6000 diffractometer operating at 40 kV and 40 mA with Cu Kα radiation (λ = 0.15418 nm). The lyophilized samples were positioned on an aluminium sample holder and measurements were taken to estimate the cellulose crystallinity, as described previously (Chen, Stipanovic, Winter, Wilson, & Kim, 2007). Crystallite dimensions were determined according to the Scherrer equation (Ramos et al., 1993).

The molecular weight distribution of both the untreated and the partially hydrolysed bacterial cellulose was determined by gel permeation chromatography (GPC) after per-carbanylation. The samples (approximately 30 mg) were dried at 60 °C in a vacuum oven, suspended in dimethyl sulfoxide (3 mL) and reacted with phenyl isocyanate (0.30 mL) for 48 h at 80 °C, under occasional stirring. The resulting mixtures were precipitated with methanol, filtered, washed thoroughly with methanol and dried under vacuum in a desiccator against phosphorus pentoxide. The samples were then solubilized in Tetrahydrofuran (THF) (1 mL) and analyzed in a Shimadzu LC10AD device, provided with a guard column and four Tosoh TSK Gel columns (7.8 × 300 mm) with exclusion limits of 4×10^7, 4×10^5, 6×10^4 and 1×10^3 units of molecular weight. THF was used as the eluting solvent at a flow rate of 1 mL min^{-1}. The elution profile was monitored by UV absorbance using a Shimadzu SPD-10A UV detector at a wavelength of 254 nm. The GPC calibration curve was generated from polystyrene standards with narrow Mw distributions. The Mark–Houwink coefficients used for calibration were $K_p = 1.18 \times 10^{-4}$ and $\alpha_p = 0.74$ for polystyrene and $K_c = 2.01 \times 10^{-5}$ and $\alpha_c = 0.74$ for cellulose tricarbanylate (Valtasaari & Saarela, 1975). The degree of polymerization (DP) of cellulose was obtained by dividing the molecular weight (M_w) of the tricarbanylated polymer by the M_w of the tricarbanyl derivate of anhydroglucose (DP = M_w/519).

Scanning electron microscopy (SEM) images were obtained in a JEOL JSM-6360 electron microscope, with acceleration voltage of 15 kV and magnification of 1000–20,000 times. The fibres were dispersed in distilled water, dropped over an aluminium sample holder, dried at 60 °C in a vacuum oven and sputtering coated with a thin gold film to avoid charge build up.

AFM images were obtained with a Shimadzu SPM 9500J3 device in tapping mode. All images (30 × 30 μm) were treated with the device's software to obtain the height profile and width of the fibres.

2.3. Preparation of the bionanocomposite films

Glycerol-plasticized bionanocomposite films were prepared from starch/bacterial cellulose aqueous suspensions by casting. Starch was dispersed in water in a concentration of 40 g L^{-1}, to which glycerol was added at a ratio of 30% (w/w) in relation to the dry starch mass. Bacterial cellulose nanofibres, treated or not with *T. reesei* endoglucanases for various incubation times, were then added at a ratio of 2.5% (w/w) relative to the dry starch mass, under strong magnetic stirring. The mixture was then heated under reflux and stirred at 90–95 °C for 30 min to ensure complete gelatinization of starch. The mixture was casted in a PVC dish and dried in a vacuum oven at 60 °C for 24 h. High temperatures and/or long drying periods without vacuum produced inhomogeneous materials with air bubbles visibly trapped in the films. Even under optimized conditions, the films showed some opacity, demonstrating that the dispersion of the cellulose nanofibres was not ideal (Ljungberg et al., 2005). The resulting films were maintained for 10 days at 43% relative humidity over a saturated K_2CO_3 solution in a desiccator at room temperature, according to ASTM E 104. Films without cellulose were produced under the same conditions for control purposes.

2.4. Characterization of the bionanocomposite films

Stripes of the bionanocomposite films were tape-glued onto an aluminium sample holder and XRPD experiments were performed under the same conditions described in item 2.3. To verify the development of crystalline patterns in the bionanocomposites,

films with and without bacterial cellulose were tested before and after conditioning in a humidity-controlled room with 43% relative humidity.

Tensile testing was carried out in an Instron 5565 tensile testing device, following the procedures outlined in the ASTM method D 882-95a. At least five replicates with 10 mm in width were tested for each sample, at a cross-head speed of 4 mm min^{-1}.

After the tensile testing, the resulting fracture surfaces were studied by SEM in a JEOL JSM-6360 electron microscope with an acceleration tension of 15 kV and a magnification of 300–5000 times.

3. Results and discussion

3.1. Mechanical properties

Fig. 1 shows the stress/strain curves of TPS films without and with reinforcement with untreated and partially hydrolyzed bacterial cellulose. In general, the mechanical properties of the reinforced nanocomposites were considerably improved in relation to the properties of TPS (Figs. 1 and 2).

Reinforcement of TPS films with untreated bacterial cellulose caused a fourfold increase in their elastic modulus and tensile strength. On average, the elastic modulus increased from 33.4 ± 4.3 to 140.6 MPa, whereas the tensile strength increased from 1.09 ± 0.39 to 4.15 MPa, as shown in Fig. 2a and b, respectively.

The incorporation of partially hydrolysed bacterial cellulose into the TPS matrix also had a substantial effect in its mechanical properties. However, the extent of this depended upon the length of the enzyme treatment with *T. reesei* endoglucanases. Both the elastic modulus and the tensile strength of the reinforced matrices increased dramatically with the incorporation of bacterial cellulose fibres that were hydrolysed for 20–60 min. From this time on, the mechanical properties of the reinforced TPS films levelled down to approximately the same properties found in the non-reinforced material. Hydrolysis for 60 min produced the best reinforcement agents for the TPS matrix. The elastic modulus of these bionanocomposites was four times higher than that of the film containing untreated fibres (140.6 ± 40.3 MPa versus 575.7 ± 166.7 MPa) and seventeen times higher than that of the plasticized starch without reinforcement (33.4 ± 4.3 MPa versus 575.7 ± 166.7 MPa). Likewise, the tensile strength almost doubled in relation to the film reinforced with untreated fibres (4.15 ± 0.66 MPa versus 8.45 ± 2.35 MPa) or increased by a factor of eight (1.09 ± 0.39 MPa versus 8.45 ± 2.35 MPa) in relation to the non-reinforced film. Additional information on the mechanical properties of these unique bionanocomposites will be presented in a forthcoming publication.

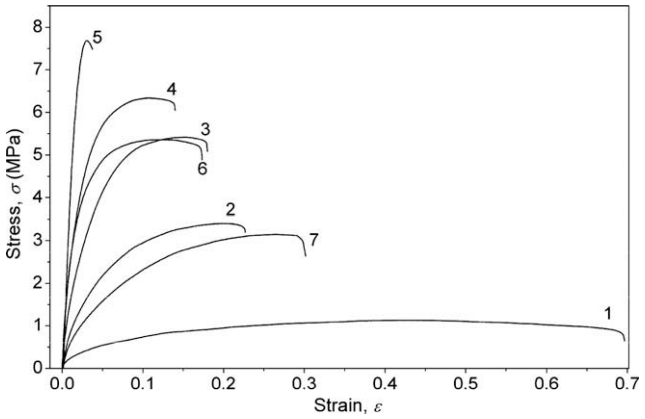

Fig. 1. Stress/strain curves of (1) TPS, (2) TPS reinforced with 2.5% (wt/wt) of untreated bacterial cellulose and TPS reinforced with 2.5% of bacterial cellulose that was treated with *Trichoderma reesei* endoglucanases for (3) 20, (4) 40, (5) 60, (6) 80 and (7) 120 min.

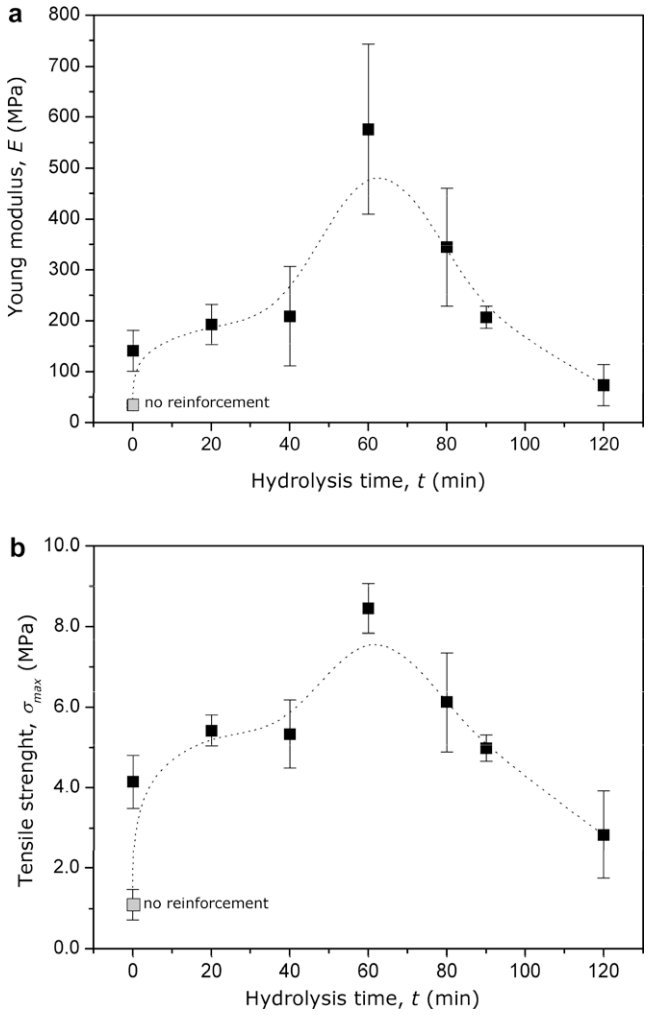

Fig. 2. Mechanical properties of the bionanocomposite films in relation to the incubation time of bacterial cellulose with *Trichoderma reesei* endoglucanases. (a) Young's or elastic modulus and (b) tensile strength. The non-reinforced TPS film is shown in gray.

The extent of enzymatic hydrolysis was evaluated by measuring the release of reducing sugars as well as by HPLC analysis of substrate hydrolysates. Table 1 shows the amount of soluble sugars (glucose and cellobiose) as determined by HPLC, as well as the mass loss observed as a result of hydrolysis.

Hydrolysis for as long as 150 min caused very little substrate mass loss as measured by the release of soluble sugars (mostly glucose and cellobiose). Similar behaviour was observed by other authors using the same enzyme system, which due to its high

Table 1
Mass loss during enzymatic hydrolysis as determined by HPLC determination.

Hydrolysis time (min)	Cellobiose (mg L^{-1})	Glucose (mg L^{-1})	Anhydroglucose equivalents (mg L^{-1})	Mass loss (wt%)
60	2.1	48.4	45.6	1.00
120	5.4	51.8	51.7	1.14
150	11.3	62.7	67.1	1.48

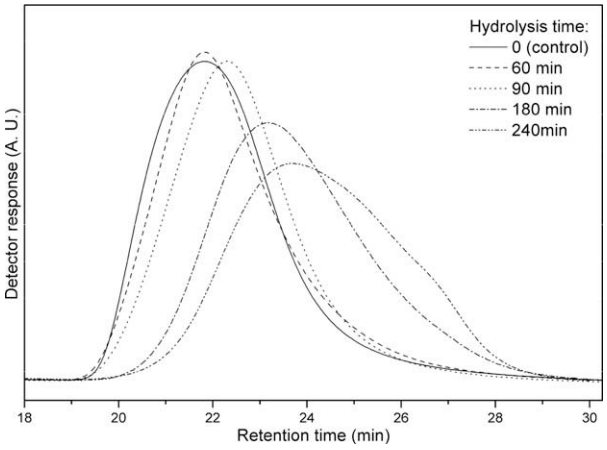

Fig. 3. GPC profiles of the per-carbanylated derivatives of bacterial cellulose before and after hydrolysis with *Trichoderma reesei* endoglucanases.

endoglucanase activity and almost negligible (if not absent) cellobiohydrolase activity causes a considerable decrease in the degree of cellulose polymerization (see below) without generating a substantial mass loss upon hydrolysis (Dufresne, 2009; Zandoná Filho et al., 2003). This behaviour was also due to the highly organized structural organization of the bacterial cellulose microfibrils, which are formed by smaller structures or elementary fibrils that are continuously segregated by the bacteria during biosynthesis. The assembly of these elementary fibrils into the microfibrils leads to the formation of regions of greater molecular organization, termed "crystallites", which are surrounded by less organized or "amorphous" regions (Iguchi, Yamanaka, & Budhiono, 2000).

Table 2
Weight average degree of polymerization (DP_w), number average degree of polymerization (DP_n) and polidispersity (DP_w/DP_n) of bacterial cellulose before and after hydrolysis with *T. reesei* endoglucanases.

Hydrolysis time (min)	DP_w	DP_n	DP_w/DP_n
0 (control)	2314	647	3.57
60	1439	553	2.60
90	1213	553	2.19
120	1199	373	3.21
180	496	218	2.28
240	430	166	2.59

According to the literature (Koizumi et al., 2008) the amorphous region occupies roughly 90% of the volume of the cellulose bundles. However, the crystallinity measurements obtained in this work (data not shown) suggest that this region corresponds to a limited amount of the total bacterial cellulose mass. These differences are probably due to the strategies used for sample preparation, which in our case included freeze-drying of the cellulosic materials after solvent exchange with *tert*-butanol (Ramos et al., 1993). Crystallinity indexes as high as those described in this work have also been reported by other authors for different samples of *A. xylinum* bacterial cellulose (Dufresne, 2009).

In light of the organization model for bacterial cellulose and because the action of the endoglucanases is more effective in the amorphous regions of the cellulose supramolecular structure (Ramos et al., 1999), it is possible that the action of the enzymes occurred more intensively in the cellulose chains located inbetween regions of higher molecular order. As well described in the literature, these

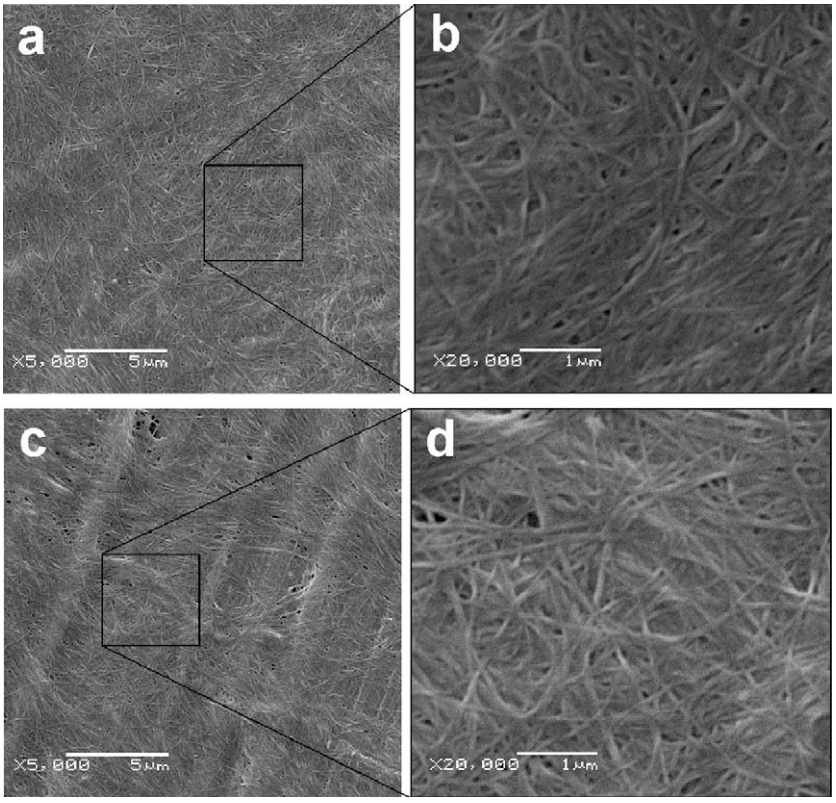

Fig. 4. Scanning electron micrograph of the untreated bacterial cellulose fibers (a and b) hydrolysated for 60 min (c and d).

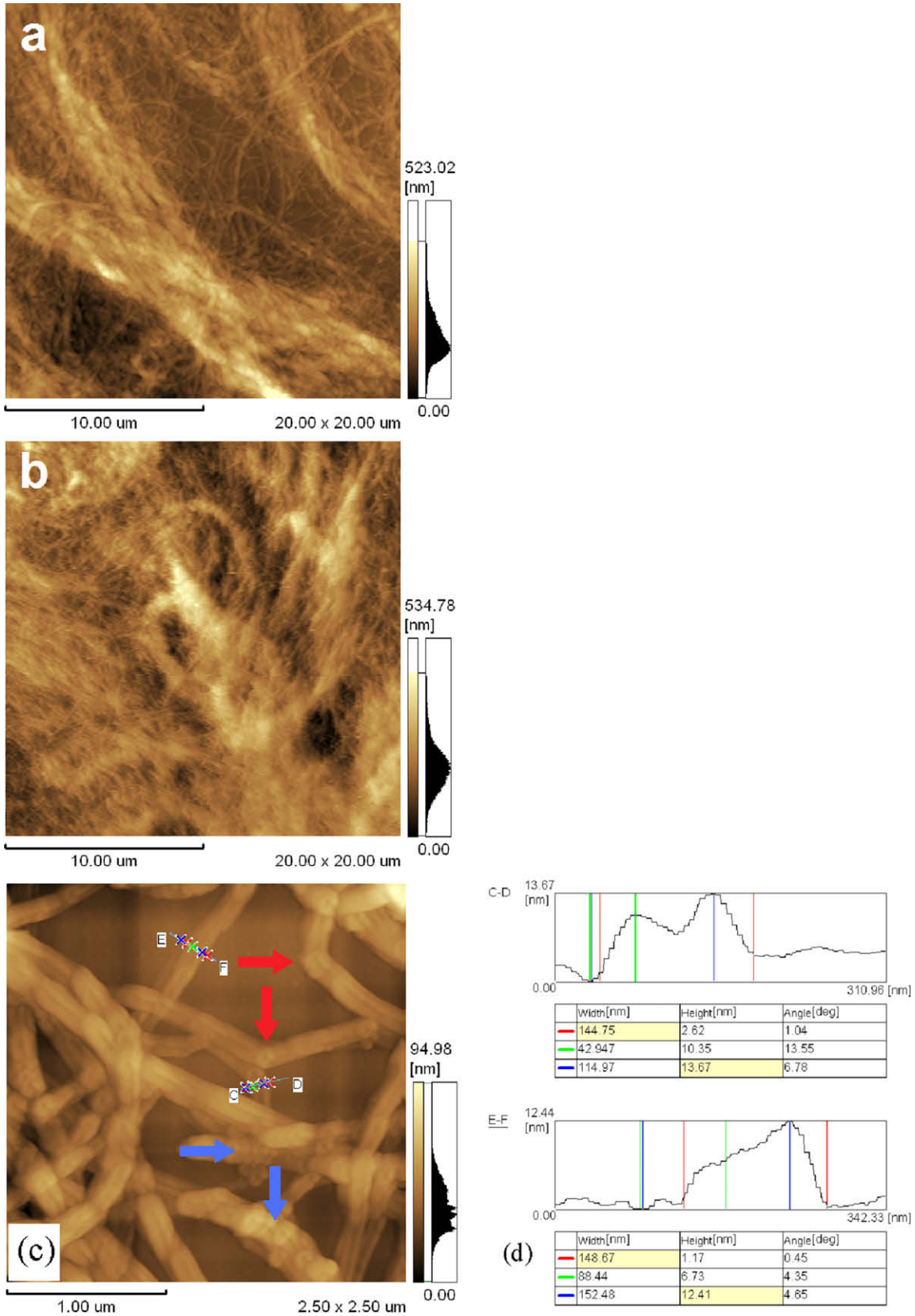

Fig. 5. AFM micrographs of bacterial cellulose (a) before, (b) after enzymatic hydrolysis for 60 min. AFM (c and d) height profiles of the original bacterial cellulose.

amorphous regions are more susceptible to attack by endoglucanases. This process results in the well-known disaggregation of the cellulose bundles (Ramos et al., 1993), freeing individual microfibrils until nanoscale structures are gradually generated.

As a result, the material becomes much more easily dispersed in the polymer matrix, thus enhancing its reinforcement properties. However, longer hydrolysis times are not desirable, as these lead to gradual hydrolysis and weakening of the crystalline regions. In fact, this critical observation partly explains the decreasing reinforcement effect of bacterial cellulose after enzymatic hydrolysis for more than 60 min.

A direct comparison of the HPLC results shown in Table 1 with the release of reducing sugars (control = 165 mg/L^{-1} of total reducing sugar and 183 mg L^{-1} of anhydroglucose; 120 min = 629 mg/L^{-1} of total reducing sugar and 699 mg L^{-1} of anhydroglucose; 240 min = 650 mg/L^{-1} of total reducing sugar and 722 mg L^{-1} of anhydroglucose) supports the interpretation discussed above. If the total reducing sugars released after 120 min were assumed to be glucose only, the total mass loss would be equivalent to 11 wt%, even if the reducing sugars present in the untreated cellulose were subtracted. This discrepancy means that the enzyme breaks down glycosidic linkages in the middle of the cellulose chains (endoglucanase mode of action), thus forming new reducing ends without a significant release of mono or disaccharides.

The comparison of these results with the typical conversion of cellulose to glucose found in acid hydrolysis, around 40% (Bondeson et al., 2006), shows the advantage of enzymatic hydrolysis in terms of fibre yield.

The degree of polymerization of bacterial cellulose was obtained by GPC of their corresponding per-carbanylated derivatives (Ramos et al., 1993, 1999). Fig. 3 shows the GPC elution profile of both untreated and partially hydrolyzed samples. All graphs were normalized by area to facilitate the observation of changes that occurred as a result of hydrolysis. Treatment of bacterial cellulose with endoglucanases caused a gradual shift of the elution band towards greater retention times, with the subsequent accumulation of low molecular weight oligomers in the reaction media.

The estimated degree of polymerization (DP) of both untreated and partially hydrolyzed bacterial cellulose is shown in Table 2.

There was a subtle decrease in cellulose DP up until 60 min of hydrolysis. After that, cellulose DP continued to decrease but at a much slower hydrolysis rate. Longer chains were cleaved in a typical endoglucanase mode of action, leading to the formation of shorter chain lengths that reassembled themselves as bacterial cel-

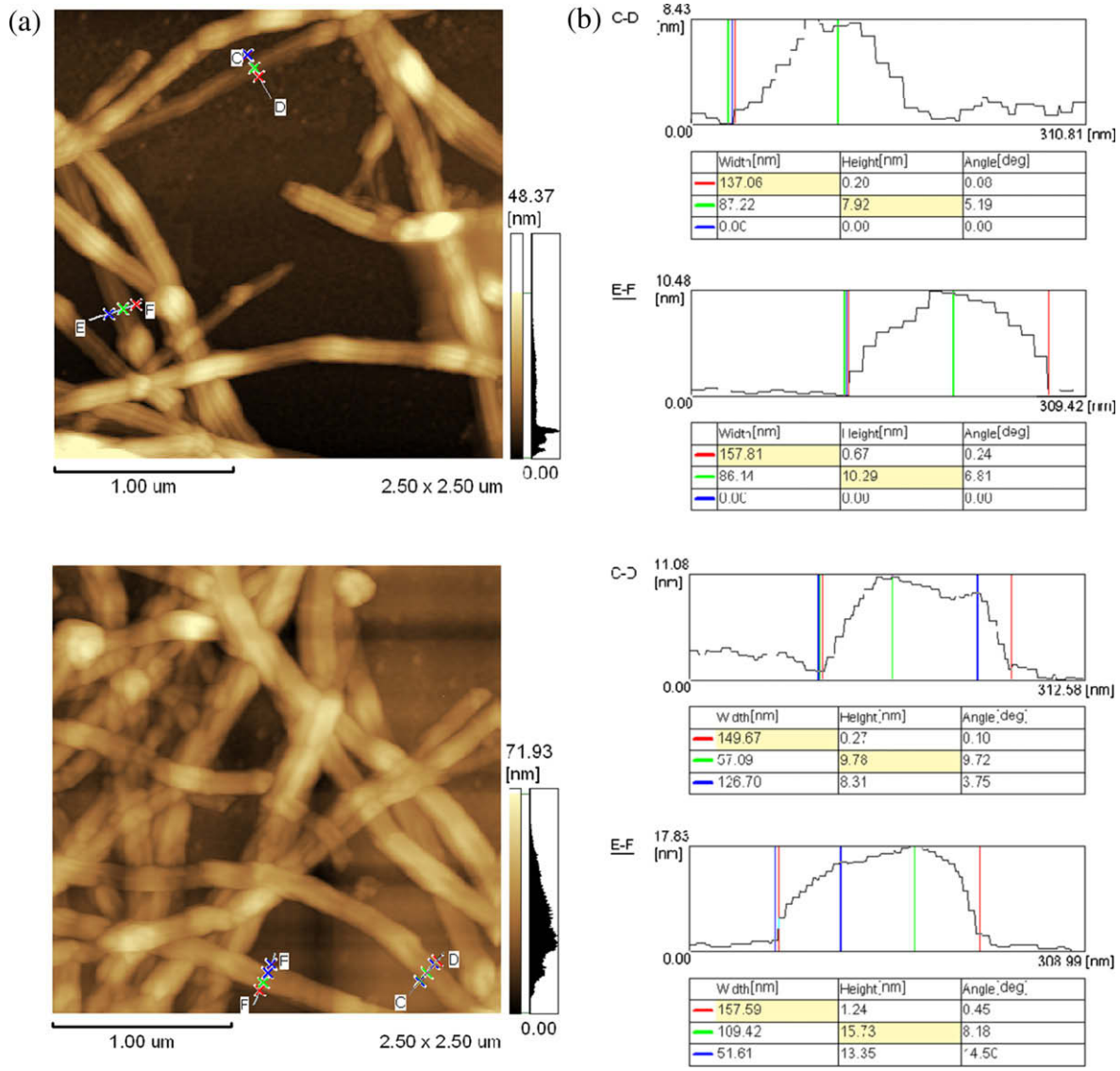

Fig. 6. AFM (a) images and (b) height profiles of bacterial cellulose before and after enzymatic hydrolysis for 60 min.

lulose nanoparticles. Endoglucanases probably attacked long chain segments that were located between the more organized elementary fibrils. Finally, the accumulation of short molecules with low DP became evident with the appearance of a shoulder in the elution profile of samples that were hydrolyzed for as long as 240 min.

The XRPD profile of bacterial cellulose did not show any significant change after partial hydrolysis with *T. reesei* endoglucanases (data not shown). Hence, hydrolysis was not able to interfere with the level of organization of the cellulose chains, in spite of their extensive loss in cellulose DP. This was confirmed by the estimation of the crystallinity index (CI) of bacterial cellulose, which remained relatively similar even after 240 min of hydrolysis (data not shown).

No changes were observed also in the size of the crystallites in any of the indexed peaks identified by XRPD. This suggests that the enzymes were not able to attack or interfere with any of the crystallographic axes of the cellulose crystallites. Unfortunately, calculation of the crystallite size in the chain direction was not possible because the corresponding XRPD peak (0 0 4) was broad and poorly defined. In this case, peak broadening might have been caused by the superposition of at least two diffraction peaks. This would explain the apparent inconsistency in the results obtained by applying the Scherrer equation to that specific direction.

Based on the available data, changes in the reinforcement capacity of the fibres could not be related to changes in cellulose crystallinity or crystalline structure. The changes imparted by hydrolysis were restricted to the less organized, amorphous regions of the bacterial cellulose supramolecular structure, therefore not affecting the structure of the elementary fibrils. Hydrolysis of the amorphous phase inbetween cellulose crystallites led to an improved dispersion of the fibres within the starch/glycerol matrix. This was probably the reason for the observed enhancement in the resulting material's mechanical properties.

3.2. Morphology of the hydrolysates

Comparison of bacterial cellulose SEM images (Fig. 4a and b) with those derived from samples that were hydrolyzed for 60 min (Fig. 4c and d) revealed no significant difference in fibre morphology, at least in the macroscopic point of view. The fibres were very regular in width, with an estimated average value of 90 nm in both samples, although charge concentration effects could have caused overestimation of these measurements. Therefore, the structural changes imparted by enzymatic hydrolysis must have occurred at a resolution level much lower than that obtained from SEM when analysis was carried out without charging, which leads to the degradation of the sample specimen.

AFM analysis of bacterial cellulose before and after enzymatic hydrolysis was much more elucidative. The untreated material (Fig. 5a) was shown to be organized in fibre bundles 2–10 μm in width. Even the individual fibres showed a tendency to aggregate into small bundles. After 60 min of enzymatic hydrolysis (Fig. 5b), the orientation of the fibres was lost and their distribution seemed almost completely random. Also, the fibres seemed to be much shorter, but precise length measurements were not possible because the image was diffused and the fibres were partially overlapped.

Higher magnification of the untreated bacterial cellulose (Fig. 5c) showed fibres with irregular surface (blue arrows)[1] and "elbows" (red arrows), in which the fibre direction changed abruptly. These features disappeared almost completely in the partially hydrolyzed fibres. Analysis of the height profiles (Figs. 5d and 6b) reveals that hydrolysis smoothens the initially sharp profile of the fibres, as if the fibre edges were cut by the concerted action of endoglucanases.

Changes in fibre morphology have been usually related to subtle increases in fibre mechanical properties (Nakagaito & Yano, 2004). The authors attributed the superior mechanical properties of microfibrillated cellulose fibres to the elimination of fibre defects that may act as crack initiators. If the irregularities observed in the original bacterial cellulose correspond to those crack initiators, an additional reinforcing mechanism may occur when the hydrolysis eliminates those regions, which are probably less organized than the rest of the fibre.

The smoothening of the fibre surface could also be a confirmation of the proposed disaggregation mechanism. The amorphous regions were not clearly observed in the AFM images because of the image broadening caused by the microscope tip width, but their disappearance was noticeable by the ease with which the tip could approach the fibre surface.

4. Conclusions

The combination of bacterial cellulose with plasticized starch proved to have much better mechanical properties than the plasticized starch alone. However, the reinforcement properties of bacterial cellulose nanofibres were considerably enhanced by an enzyme treatment using *T. reesei* endoglucanases. The enzymatic treatment also had the advantage of causing less material loss in comparison to other nanofibre production processes, such as acid hydrolysis or mechanical fibrillation.

The increased reinforcement capacity of the enzyme treated fibres was related to two different mechanisms. The first was the elimination of less organized regions between the fibres that entangled them to each other in the original material, thus allowing a much better dispersion of the reinforcing agent into the starch matrix. The second was the reduction of defects in the surface of the fibres that could act as crack propagators.

This first article discusses the properties of the bionanocomposites in terms of changes in the structure of the reinforcing material. A second contribution will describe more accurately the observed changes in mechanical properties and relate them to the interactions between the starch matrix and the bacterial cellulose nanofibres.

Acknowledgements

We gratefully acknowledge the financial support of the Brazilian research funding agencies CNPq, Capes and FINEP. We are especially indebted to the Centro de Microscopia Eletrônica – CME/UFPR for providing the SEM measurements, to Membracel Produtos Tecnológicos Ltda, Corn Products Brasil and Röhm Enzyme Finland Oy for kindly supplying the bacterial cellulose, corn starch and enzymes, respectively.

References

Abe, K., Iwamoto, S., & Yano, H. (2007). Obtaining cellulose nanofibres with a uniform width of 15 nm from wood. *Biomacromolecules, 8*, 3276–3278.

Àngles, M. N., & Dufresne, A. (2000). Plasticized starch/tunicin whiskers nanocomposites. 1. Structural analysis. *Macromolecules, 33*, 8344–8353.

Avérous, L., Frigant, A., & Moro, L. (2001). Plasticized starch–cellulose interactions in polysaccharide composites. *Polymer, 42*, 6565–6572.

Bondeson, D., Mathew, A., & Oksman, K. (2006). Optimization of the isolation of nanocrystals from microcrystalline cellulose by acid hydrolysis. *Cellulose, 13*, 171–180.

Chaplin, M. F., & Kennedy, J. F. (1994). *Carbohydrate analysis* (2nd ed.). New York: Oxford University Press.

Chen, B., & Evans, J. R. (2005). Thermoplastic starch–clay nanocomposites and their characteristics. *Carbohydrate Polymers, 61*(4), 455–463.

[1] For interpretation of the references to colour in this text, the reader is referred to the web version of this article.

Chen, Y., Stipanovic, A. J., Winter, W. T., Wilson, D. B., & Kim, Y.-J. (2007). Effect of digestion by pure cellulases on crystallinity and average chain length for bacterial and microcrystalline celluloses. *Cellulose, 14*, 283–293.

Dufresne, A. (2009). In S. Thomas & L. A. Pothan (Eds.), *Natural fibre reinforced polymer composites: From macro to nanoscale* (pp. 142–170). Philadelphia: Old City Publishing's.

Henriksson, M., Henriksson, G., Berglund, L. A., & Lindström, T. (2007). An environmentally friendly method for enzyme-assisted preparation of microfibrillated cellulose (MFC) nanofibres. *European Polymers Journal, 43*, 3434–3441.

Iguchi, M., Yamanaka, S., & Budhiono, A. (2000). Bacterial cellulose – A masterpiece of nature's arts. *Journal of Materials Science, 35*, 261–270.

Koizumi, S., Yue, Z., Tomita, Y., Kondo, T., Iwase, H., Yamaguchi, D., et al. (2008). Bacterium organizes hierarchical amorphous structure in microbial cellulose. *The European Physical Journal E, 26*, 137–142.

Ljungberg, N., Bonini, C., Bortolussi, F., Boisson, C., Heux, L., & Cavaillé, J. Y. (2005). New nanocomposites materials reinforced with cellulose whiskers in atatic polypropylene: Effect of surface and dispersion characteristics. *Biomacromolecules, 6*, 2732–2739.

López-Rubio, A., Lagaron, J. M., Ankersfors, M., Lindström, T., Nordqvist, D., Mattozzi, A., et al. (2007). Enhanced film forming and film properties of amylopectin using micro-fibrillated cellulose. *Carbohydrate Polymers, 68*, 718–727.

Malainine, M. E., Mahrouz, M., & Dufresne, A. (2005). Thermoplastic nanocomposites based on cellulose microfibrils from *Opuntia ficus-indica* parenchyma cell. *Composites Science and Technology, 65*, 1520–1526.

Mathew, A. P., & Dufresne, A. (2002). Morphological investigation of nanocomposites from sorbitol plasticized starch and tunicin whiskers. *Biomacromolecules, 3*, 609–617.

Nakagaito, A. N., & Yano, H. (2004). The effect of morphologial changes from pulp fiber towards nano-scale fibrillated cellulose on the mechanical properties of high-strength plant fiber based composites. *Applied Physics A, 78*, 547–552.

Okada, A., Kawasumi, M., Kurauchi, T., & Kamigaito, O. (1987). Synthesis and characterization of a nylon 6-clay hybrid. *American Chemical Society, Polymer Preprints, Division of Polymer Chemistry, 28*, 447–448.

Orts, W. J., Shey, J., Imam, S. H., Glenn, G. M., Guttman, M. E., & Revol, J. F. (2005). Application of cellulose microfibrils in polymer nanocomposites. *Journal of Polymer and the Environment, 13*(4), 301–306.

Ramos, L. P., & Fontana, J. D. (2004). In J. F. T. Spencer & A. L. R. Spencer (Eds.), *Methods in biotechnology: Environmental biology: Methods in protocols*. London: Humana Press.

Ramos, L. P., Nazhad, M. M., & Saddler, J. N. (1993). Effect of enzymatic hydrolysis on the morphology and fine structure of pretreated cellulosic residues. *Enzyme and Microbial Technology, 15*, 821–831.

Ramos, L. P., Zandoná Filho, A., Deschamps, F. C., & Saddler, J. N. (1999). The effect of *Trichoderma* cellulases on the fine structure of a bleached softwood kraft pulp. *Enzyme and Microbial Technology, 24*, 371–380.

Satyanarayana, K. G., Arizaga, G. G. C., & Wypych, F. (2009). Biodegradable composites based on lignocellulosic fibres – An overview. *Progress in Polymer Science, 34*, 982–1021.

Stael, G. C., Tavares, M. I. B., & D'Almeida, J. R. M. (2001). Impact behavior of sugarcane bagasse waste–EVA composites. *Polymer Testing, 20*(8), 869–872.

Suominen, P. L., Mäntylä, A. L., Karhunen, T., Hakola, S., & Nevalainen, H. (1993). High frequency one-step gene replacement in *Trichoderma reesei*. II. Effects of deletions of individual cellulase genes. *Molecular and General Genetics, 241*, 523–530.

Tjong, S. C. (2006). Structural and mechanical properties of polymer nanocomposites. *Materials Science and Engineering Reports, 53*, 73–197.

Usuki, A., Kojima, Y., Kawasumi, M., Okada, A., Fukushima, Y., Kurauchi, T., et al. (1993). Synthesis of nylon 6-clay hybrid. *Journal of Materials Research, 8*(5), 1179–1184.

Usuki, A., Kojima, Y., Kawasumi, M., Okada, A., Kurauchi, T., & Kamigaito, O. (1990). Characterization and properties of nylon 6. Clay hybrid. *American Chemical Society, Polymer Preprints, Division of Polymer Chemistry, 31*, 651–652.

Valtasaari, L., & Saarela, K. (1975). Determination of chain length distribution of cellulose by gel permeation chromatography using the tricarbanilate derivative. *Paperi ja Puu, 57*, 5–10.

Wilhelm, H. M., Sierakowski, M. R., Souza, G. P., & Wypych, F. (2003). Starch films reinforced with mineral clay. *Carbohydrate Polymers, 52*, 101–110.

Yu, L., Dean, K., & Li, L. (2006). Polymer blends and composites from renewable resources. *Progress in Polymer Science, 31*, 576–602.

Zandoná Filho, A., Cancelier, P. D., Siika-Aho, M., & Ramos, L. P. (2003). In S. Mansfield & J. N. Saddler (Eds.), *Application of enzymes to lignocellulosics. ACS symposium series* (Vol. 855, pp. 287–303). Orlando: American Chemical Society.

Zhao, R., Torley, P., & Halley, P. J. (2008). Emerging biodegradable materials: Starch- and protein-based bio-nanocomposites. *Journal of Materials Science, 43*, 3058–3071.